Adsorption and Decomposition of Acetylene on Planar and Faceted Ir(210)

Wenhua Chen,[†] Ivan Ermanoski,[†] Qifei Wu,[‡] and T. E. Madey*[,†,‡]

Department of Physics and Astronomy, Department of Chemistry, and Laboratory for Surface Modification, Rutgers, The State University of New Jersey, Piscataway, New Jersey 08854

Henry H. Hwu and Jingguang G. Chen

Center for Catalytic Science and Technology (CCST), Department of Materials Science and Engineering, University of Delaware, Newark, Delaware 19716

Received: November 22, 2002; In Final Form: March 12, 2003

The adsorption and reaction of acetylene on both planar and faceted Ir(210) have been studied utilizing temperature-programmed desorption (TPD), Auger electron spectroscopy (AES), low-energy electron diffraction (LEED), and high-resolution electron energy loss spectroscopy (HREELS). Following adsorption of C_2H_2 at 300 K or 100 K, TPD data indicate that H_2 is the dominant desorption product, and that decomposition of adsorbed C_2H_2 occurs in a stepwise fashion. Multiple carbon-containing species are formed on Ir(210) upon adsorption of acetylene at high coverage, which are different from those formed at low coverage. Our HREELS results show that the dominant surface hydrocarbon species formed at high coverage are mainly acetylide and ethylidyne while acetylide dominates at low coverage. In contrast to reaction measurements on an Ir organometallic complex that catalyzes cyclization of C_2H_2 to C_6H_6, no evidence for the cyclization reaction is found on Ir(210). The results are compared with adsorption and decomposition of C_6H_6 on Ir(210); as for C_2H_2, the dominant desorption product is H_2, but there are differences in the reaction sequence. In addition, evidence has been found in TPD measurements for structure sensitivity in decomposition of acetylene over the clean faceted Ir(210) surface versus the clean planar Ir(210) surface, which is attributed to nanometer scale structures on the faceted surface. The HREELS data give complementary information to TPD and AES results and provide insights into the reaction mechanisms for acetylene surface chemistry.

1. Introduction

Acetylene reactions over transition metal surfaces have attracted considerable interest because of their relevance to many important catalytic reactions. One of the reaction pathways, the cyclization of acetylene to benzene ($C_2H_2 \rightarrow C_6H_6$),[1−8] is extremely structure sensitive. Certain surfaces, such as Pd(111)[1−3] and Cu(110),[4,5] are highly active toward cyclization of acetylene, whereas Pd(110)[2,9] is less active for cyclization of acetylene. A summary of Pd-catalyzed cyclization of acetylene from ultrahigh vacuum (UHV) to high pressure[10] and a review of cyclization of acetylene to benzene on transition metal surfaces including single crystals, supported particles, and bimetallic surfaces[11] are available. Other acetylene reaction pathways include self-hydrogenation of acetylene to form ethylene ($C_2H_2 \rightarrow C_2H_4$)[1,12] and decomposition of acetylene to form hydrogen ($C_2H_2 \rightarrow H_2$) and atomic carbon.[9,13−22]

There is evidence from temperature-programmed desorption (TPD) measurements for structure sensitivity in acetylene reactions to form benzene and ethylene over bimetallic Pd/W surfaces (planar Pd/W(111), faceted Pd/W(111), and extended planar Pd/W(211)).[12] These measurements also demonstrate clearly that acetylene reactions over bimetallic Pd/W surfaces exhibit size effects on the nanometer scale. W(111) is an atomically rough and morphologically unstable surface. When W(111) is covered by one physical monolayer (ML) of Pd and annealed to temperatures higher than 700 K, the initially planar surface becomes faceted with three-sided pyramidal facets having {211} faces with nanometer dimensions; facet size increases with annealing temperature.[23,24]

As a part of our ongoing project to study the morphological stability of metal surfaces covered by various adsorbates and size effects on acetylene reactions, we extend our studies from the body-centered cubic (bcc) W(111) surface to the face-centered cubic (fcc) Ir(210) surface, which is being used in this work. The atomically rough fcc Ir(210) surface (four layers exposed) is similar to the bcc W(111) surface (three layers exposed) in structure but with reduced symmetry (C_{1h} or *m* symmetry, i.e., mirror plane). The top views of these two surfaces are compared in Figure 1. Recently, we discovered that two different kinds of catalytic surfaces can be prepared from Ir(210): the clean planar Ir(210) and the clean faceted Ir(210). The clean faceted Ir(210) surface can be routinely prepared from planar Ir(210) in situ,[25,26] indicating that Ir(210) is an excellent candidate substrate to study structure sensitive reactions because traditional way to study structure sensitive reaction involves reaction studies using different single-crystal surfaces of different surface structure, which needs to switch from sample to sample. Nanometer scale facets having {311} and {110} orientations can be formed on Ir(210) upon heating in O_2 at $T > 600$ K; oxygen can be removed from the surface at 400 K by heating in H_2 to generate a clean faceted surface.

Auger peak profiles in Auger electron spectroscopy (AES) contain information about the chemical environment of adsorbed atoms and molecules.[27] Carbon atoms in different chemical configurations, e.g., SiC, graphite,[28] Ni_3C,[29] TiC, VC, Cr_3C,[30] and gaseous hydrocarbons (CH_4, C_2H_2 and C_2H_4)[31] exhibit differences in both Auger line shape and associated fine

[†] Department of Physics and Astronomy, and Laboratory for Surface Modification.

[‡] Department of Chemistry and Laboratory for Surface Modification.

* Corresponding author. E-mail: madey@physics.rutgers.edu; Fax: 732-445-4991.

10.1021/jp0224721 CCC: $25.00
Published on Web 05/10/2003

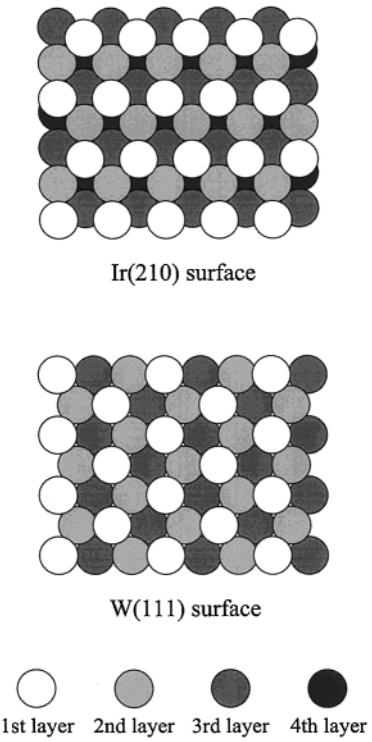

Figure 1. Top view of Ir(210) (fcc) surface and W(111) (bcc) surface: hard-sphere bulk truncation models.

structure. We make use of Auger line shapes in the present work to provide new information about the surface chemistry of acetylene on Ir. In addition, high-resolution electron energy loss spectroscopy (HREELS)[20,32,33] is a powerful technique for characterizing adsorbed species and can be used to identify the geometry of adsorbed molecules and their reaction products. The HREELS data in this work provide complementary information to AES and TPD results. An Ir organometallic complex is reported to catalyze cyclization of acetylene,[34] although such a reaction pathway was not found on Ir(111) and Ir(755) surfaces, which decompose acetylene to produce hydrogen and atomic carbon.[35] To date, no previous study of surface chemistry on the Ir(210) crystal surface has been reported. This work is a background study for studying acetylene reactions on bimetallic surfaces based on Ir substrates. We intend to search for metal film-induced faceting of Ir(210) and determine if metal/Ir surfaces exhibit structure sensitivity and size effects in acetylene surface chemistry, which is observed to occur on planar and faceted Pd/W surfaces.[12]

This paper is organized as follows. After a description of the experimental procedures, the H_2 TPD data from H_2, C_2H_2-, and C_6H_6-covered Ir(210) surface, as well as data for C_2H_2-covered faceted Ir(210) surface, are presented. This is followed by surface characterization at different acetylene coverages and at different stages of the reaction using AES, LEED, and HREELS. The discussion emphasizes the determining role of surface reactive intermediates in the thermal decomposition of acetylene, which occurs in a stepwise fashion, and evidence for structure sensitivity in decomposition of acetylene over the planar and faceted Ir(210) surfaces. The similarity and difference in reactivity of the Ir(210) surface toward acetylene and benzene as well as comparison with other iridium crystal faces are also discussed.

2. Experimental Section

The TPD experiments were performed at Rutgers University in a UHV chamber with a base pressure below 1×10^{-10} Torr.[36,37] This chamber is equipped with instrumentation for Auger electron spectroscopy (AES), low-energy electron diffraction (LEED), and a quadruple mass spectrometer (QMS). For the AES measurements, a double-pass cylindrical mirror analyzer and a grazing incidence electron gun are employed. Typically, the electron beam used for Auger excitation is $\sim$1.5 μA at 3 KV. LEED measurements using the four-grid optics are used to characterize the structures of planar and faceted Ir(210). The QMS is used for monitoring background residual gases, checking the purity of gases for dosing, and detecting desorbed species from the sample surface during TPD measurements.

The HREELS measurements were made at University of Delaware in a previously described UHV system with a base pressure below 8×10^{-10} Torr,[38] which contains AES, LEED, QMS, and HREELS. The HREELS spectrometer (LK 3000) was operated at an electron energy of 6.0 eV with a typical resolution between 42 and 50 cm^{-1}. All spectra were recorded with the sample held at 90 K.

The same Ir(210) crystal was used in both laboratories; it is an oval disk of $\sim$10 mm average diameter with a thickness of $\sim$1 mm. The sample mounting and cleaning procedures at Rutgers are different from those at Delaware. At Rutgers, the sample is spot-welded to two Re ribbon leads (the width tapers from 4 mm to a value of 1 mm at the sample; the thickness is 0.1 mm and the length is 13 mm) that are attached to the Mo rods for support and resistive heating.[25,26] For cleaning, the Ir sample is heated by electron beam bombardment from a W filament behind the Ir crystal, while sample heating during TPD measurements (typically 5 K/s heating rate) is achieved by resistive heating, i.e., passing DC current through the sample. The sample can be cooled to 100 K by liquid nitrogen (LN) and heated to 1300 K by resistive heating or 2000 K by e-beam heating. The sample temperature is measured using a W$-$5%Re/W$-$26%Re thermocouple that is spot-welded to the back of the sample. At Delaware, the sample was spot-welded to two tantalum wires for support and resistive heating and a type K thermocouple is used to monitor the sample temperature. The sample is cleaned by sputtering and annealing to $\leq$1200 K as described below. The sample can be fast cooled to 90 K.

At Rutgers, different sample cleaning procedures are employed depending on whether the normal *clean PLANAR* Ir(210) surface or *oxygen-covered FACETED* Ir(210) surface or *clean FACETED* Ir(210) surface is to be prepared. The clean planar Ir(210) surface is obtained by cycles of flashing the sample to 1700 K in O_2 (5×10^{-8} Torr) to remove surface carbon contamination followed by flashing the sample to 1700 K in UHV to remove surface oxygen. We generate an oxygen-covered nanoscale-faceted Ir(210) surface by flashing clean planar Ir(210) in O_2 (5×10^{-8} Torr) to high temperature ($\sim$1700 K) and then cooling in O_2 to room temperature or 100 K before pumping away O_2. The clean faceted Ir(210) surface is generated by removing surface oxygen from oxygen-covered faceted Ir(210) surface via a catalytic reaction with H_2: annealing the sample in H_2 (5×10^{-9} Torr) at 400 K for 3.5 min followed by annealing the sample in UHV at 400 K for 2 min. The surface cleanliness and structure are verified using AES, TPD, and LEED. The facet orientations are {311} and {110} as determined in a LEED analysis.[25,26]

At Delaware, the clean planar Ir(210) surface is generated by cycles of Ne^+ sputtering (3 KV and 6$-$8 μA sample current) at 1000 K and annealing at 1150 K for 5 min. The clean faceted Ir(210) surface is generated through catalytic reaction with H_2 at 400 K to remove surface oxygen from oxygen-covered faceted

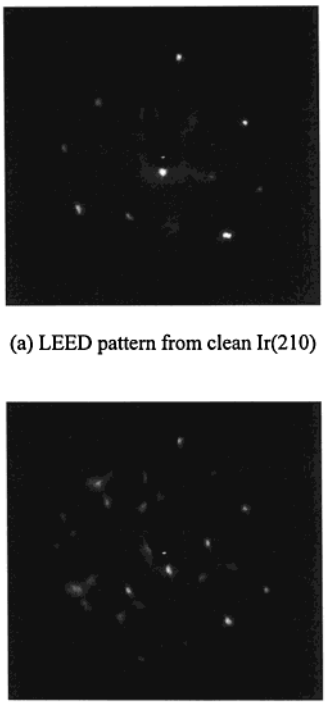

Figure 2. LEED patterns from (a) the clean planar Ir(210) surface and (b) the clean faceted Ir(210) surface at an incident electron energy of 75 eV.

Ir(210), which is generated by flashing clean planar Ir(210) in O_2 to 1200 K and then cooling in O_2.

The acetylene (99.96% purity, from Matheson) is purified by passing it through a dry ice/acetone cooled trap, while the benzene (99.99% purity, from Aldrich) is purified by several freeze−pump−thaw cycles.[11] The purity of both acetylene and benzene are verified with the QMS prior to use in the UHV chamber. Oxygen (99.99%, from Matheson) and hydrogen (Research grade, from Matheson) are used without further purification. All dosing is carried out by back-filling the chamber; all exposures are in langmuirs (1 langmuir = 10^{-6} Torr s) and are uncorrected for ion gauge sensitivities.

3. Results

3.1. Thermal Stability of Faceted Ir(210). A LEED pattern from clean planar Ir(210) with (1 × 1) structure is shown in Figure 2a. When the surface is annealed to high temperatures (2000 K) and cooled to 300 K, the surface is planar; when the energy of the normally incident electron beam is increased, all the LEED spots move and converge toward the center (00) beam, which is characteristic of a planar surface. In addition, the surface remains planar when covered with 3 langmuirs of C_2H_2 and annealed to higher temperatures. All this indicates that annealing in UHV or coverage by adsorbate acetylene does not induce faceting of Ir(210). However, adsorbed oxygen can induce faceting of Ir(210): nanometer-scale pyramid-like facets are formed on the initially planar surface when clean planar Ir(210) is exposed to more than ∼0.9 langmuir of oxygen and annealed to $T > 600$ K.[25,26] Figure 2b shows a characteristic LEED pattern from the clean faceted Ir(210) surface: extra LEED spots appear compared to the clean planar surface at the same incident energy, and when the incident energy is increased, all the LEED spots move and converge toward fixed spots that correspond to the specularly reflected beams of {311} and (110) facets.[26] The clean faceted Ir(210) surface converts to the clean planar Ir(210) surface upon heating above 600 K (5 K/s), i.e., the clean faceted Ir(210) surface is stable only to 600 K. But when 3 langmuirs of C_2H_2 is adsorbed on the clean faceted Ir(210) surface, the acetylene-covered faceted surface converts to the acetylene-covered planar surface upon heating above 700 K (5 K/s), indicating that adsorbed acetylene stabilizes the facets.

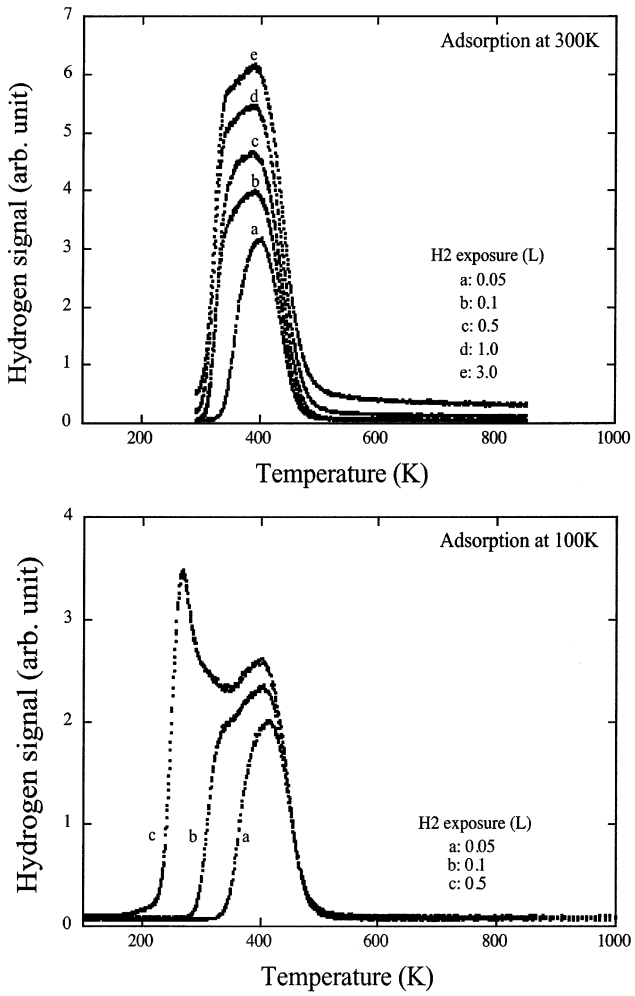

Figure 3. Temperature-programmed desorption spectra of H_2 from Ir(210) surface preexposed to different exposures of H_2 at 300 and 100 K, respectively.

3.2. Adsorption and Desorption. Hydrogen is the major desorption product resulting from the decomposition of many hydrocarbons on catalytic surfaces. The direct comparison of H_2 TPD spectra from hydrogen-covered Ir(210) surface with those from the hydrocarbon-covered Ir(210) surface help us ascertain whether the hydrogen desorbed from the hydrocarbon-covered Ir(210) surface is reaction-rate limited or desorption-rate limited. We begin by presenting TPD spectra of H_2 from hydrogen-covered Ir(210) followed by those from hydrocarbon-covered Ir(210).

3.2.1. H_2 on Ir(210). We measure TPD spectra of H_2 following adsorption of different exposures of H_2 on Ir(210) at 300 and 100 K, respectively. Figure 3 displays TPD spectra of H_2 as a function of H_2 exposure. For adsorption at 300 K and at 0.05 langmuir exposure, a single symmetric desorption peak is observed centered around 400 K. A shoulder at ∼340 K starts to appear when exposure increases and becomes saturated quickly. For adsorption at 100 K, in addition to the high-temperature desorption peak (∼410 K), a sharp peak at ∼270 K is seen for a dose of 0.5 L H_2 on Ir(210), demonstrating that there are at least two distinct binding states of hydrogen. Note

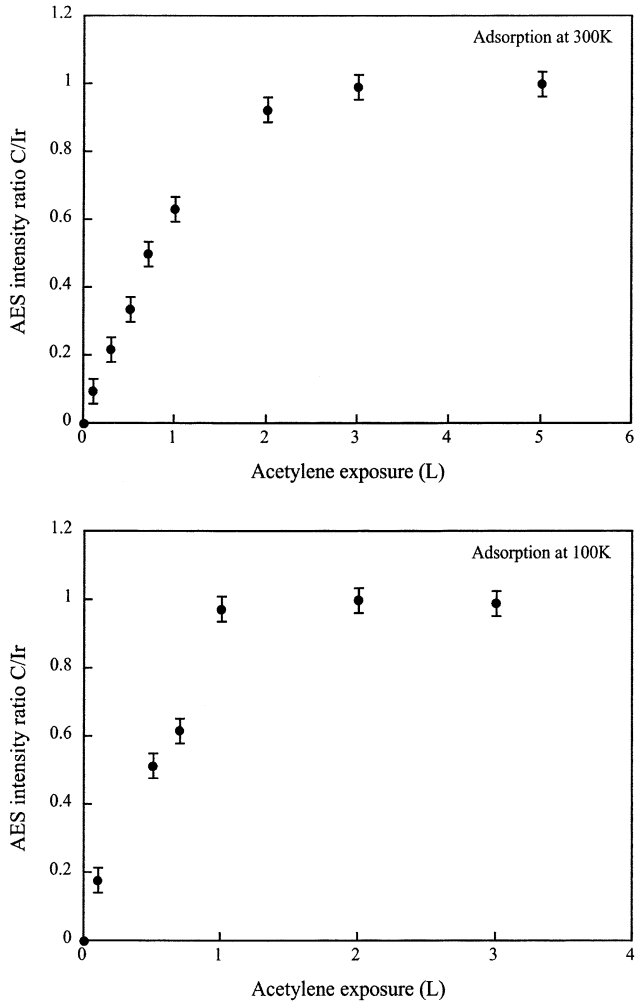

Figure 4. Normalized AES intensity ratio of C(272 eV):Ir(171 eV) as a function of exposure of C_2H_2 on Ir(210) surface at 300 and 100 K, respectively.

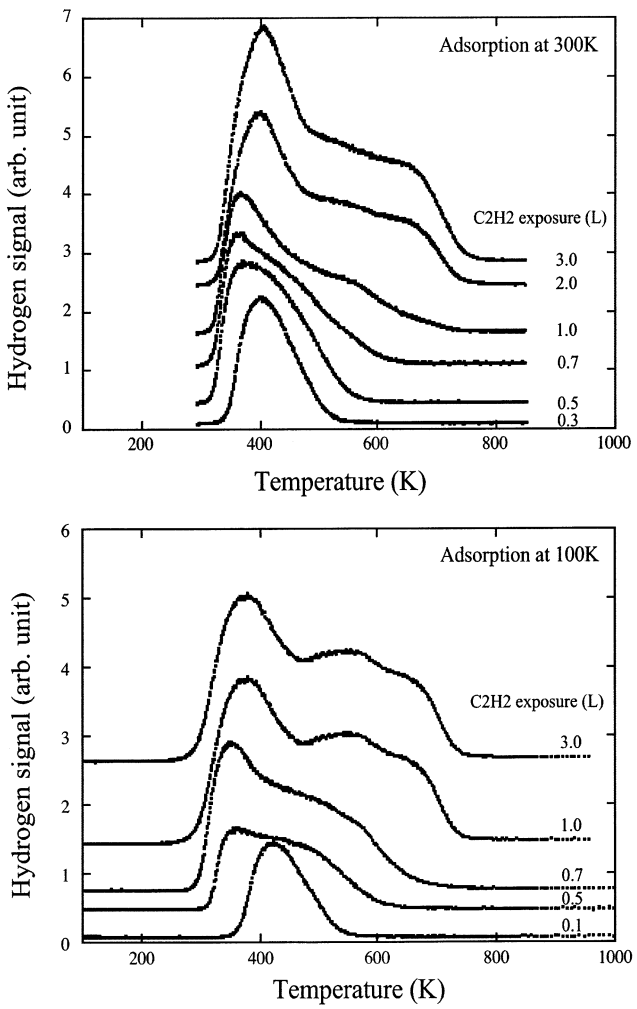

Figure 5. Temperature-programmed desorption spectra of hydrogen for different exposures of acetylene on clean Ir(210) surface at 300 and 100 K, respectively.

that all adsorbed H_2 desorbs completely at ~500 K; this is the key result we discuss later to determine whether the desorbed H_2 from C_2H_2- or C_6H_6-covered Ir(210) during TPD is reaction-rate limited or desorption-rate limited. A detailed study of hydrogen adsorption states and hydrogen desorption kinetics on Ir(210) will be reported elsewhere.[39]

3.2.2. C_2H_2 on Planar Ir(210). Figure 4 shows the AES carbon uptake curve, i.e., AES peak-to-peak intensity ratio of C(272 eV) to Ir(171 eV) as a function of acetylene exposure on the clean Ir(210) surface at 300 K (upper part) and 100 K (lower part), respectively. Each data point corresponds to a fresh dose of C_2H_2 onto an initially clean Ir(210) surface. This shows that the saturation exposure is ~3 langmuirs at 300 K and ~1 langmuir at 100 K, which is consistent with TPD results described below. However, 3 langmuir doses are used in all experiments to ensure the saturation dose of C_2H_2 on Ir(210) at both 300 and 100 K.

When clean Ir(210) is exposed to various coverages of acetylene at 300 or 100 K and then heated, the dominant desorption product (>99%) is H_2 as a result of thermal decomposition of acetylene. In particular, no C_6H_6 desorption product is found during TPD following adsorption of a saturation coverage (3 langmuir dose) of C_2H_2 on Ir(210) at 300 or 100 K, indicating that Ir(210) is inactive to the acetylene cyclization reaction. This is in contrast to reaction measurements over an Ir organometallic complex that catalyzes cyclization of acetylene.[34]

Figure 5 contains a series of TPD spectra of H_2 for different exposures of acetylene on Ir(210) at 300 K (upper part) and 100 K (lower part), respectively. Two distinct features in the TPD spectra of H_2 have been observed. At lower exposures ($\leq$0.7 langmuir of C_2H_2), the main H_2 peak on the low-temperature side (<420 K) initially moves to lower temperatures with increasing exposure of C_2H_2 while it shifts to higher temperatures at higher exposures (>0.7 langmuir of C_2H_2). Moreover, several new H_2 peaks develop on the high-temperature side at higher exposures (>0.7 langmuir of C_2H_2). The differences in the TPD spectra of H_2 for H_2/Ir(210) from those for C_2H_2/Ir(210) indicate that the desorption of H_2 from C_2H_2 on Ir(210) is reaction-rate limited. Note that the dominant features of the H_2 TPD spectra in Figure 5 for the two cases (300 and 100 K adsorption) are very similar, although the onset decomposition temperature is slightly lower in the case of 100 K adsorption. This suggests that the acetylene reaction mechanism over Ir(210) surface for adsorption at 100 K should be similar to that for adsorption at 300 K.

The TPD spectra of hydrogen accompanying decomposition of acetylene are essentially unchanged for all C_2H_2 exposures $\geq$3 langmuirs at 300 K and for all C_2H_2 exposures $\geq$1 langmuir at 100 K. This indicates that exposures of 3 langmuirs of C_2H_2 on Ir(210) at 300 K and 1 langmuir of C_2H_2 on Ir(210) at 100 K produce saturation coverage of adsorbed C_2H_2 on Ir(210) at 300 and 100 K, respectively, consistent with AES measurements.

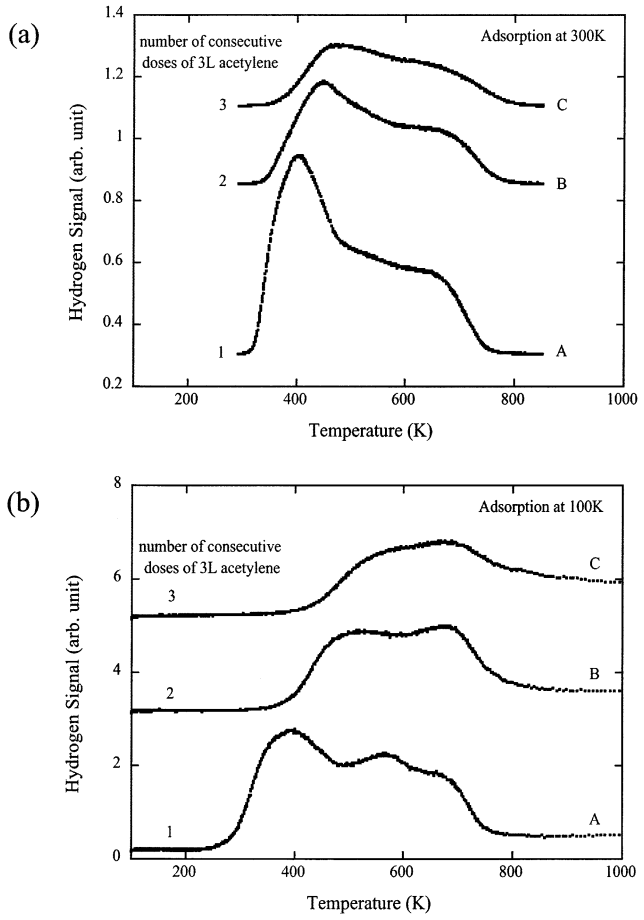

Figure 6. Temperature-programmed desorption spectra of H_2 following adsorption of consecutive doses of 3 langmuirs of C_2H_2 on Ir(210) surface at 300 and 100 K, respectively.

Figure 6 displays the TPD spectra of H_2 following three consecutive doses of 3 langmuirs of C_2H_2 on Ir(210) to show the effects of self-poisoning by acetylene thermal decomposition products; no oxygen treatment was used to remove residual C deposits between experiments. The successive spectra correspond to 3 langmuirs of C_2H_2 on different surfaces, i.e., clean Ir(210) and Ir(210) covered with different amount of carbon deposit. We start by dosing 3 langmuirs of C_2H_2 onto clean planar Ir(210) at 300 K and measuring the H_2 TPD spectrum A in the upper part of Figure 6, stopping at 850 K. After it is cooled to 300 K, the surface is exposed again to 3 langmuirs of C_2H_2, and spectrum B is measured. After measuring B, we dose 3 langmuirs of C_2H_2 again and measure spectrum C. The bottom part shows a similar series of dose/TPD measurements for 3 langmuir exposures at 100 K, with the maximum TPD temperature of 1000 K. In each case, the H_2 TPD spectra are different from each other on the three surfaces in both peak profile and peak area, indicating the surfaces have different surface reactivity. As the number of dose/TPD cycles increases, the reactivity of the surface decreases rapidly as seen by the reduction of the H_2 TPD peak area. The intensity of the main H_2 peak below 500 K drops much faster than others as the surface reactivity decreases, especially for adsorption at 100 K. This is attributed to a gradual surface site-blocking as a result of increased carbon deposit due to thermal decomposition of acetylene.

3.2.3. C_6H_6 on Planar Ir(210). For comparison with C_2H_2 on Ir(210), we studied the adsorption of C_6H_6 on Ir(210) at 300 K. The saturation exposure of C_6H_6 on Ir(210) at 300 K is ~3 langmuirs, and the dominant desorption product (>99%) is H_2.

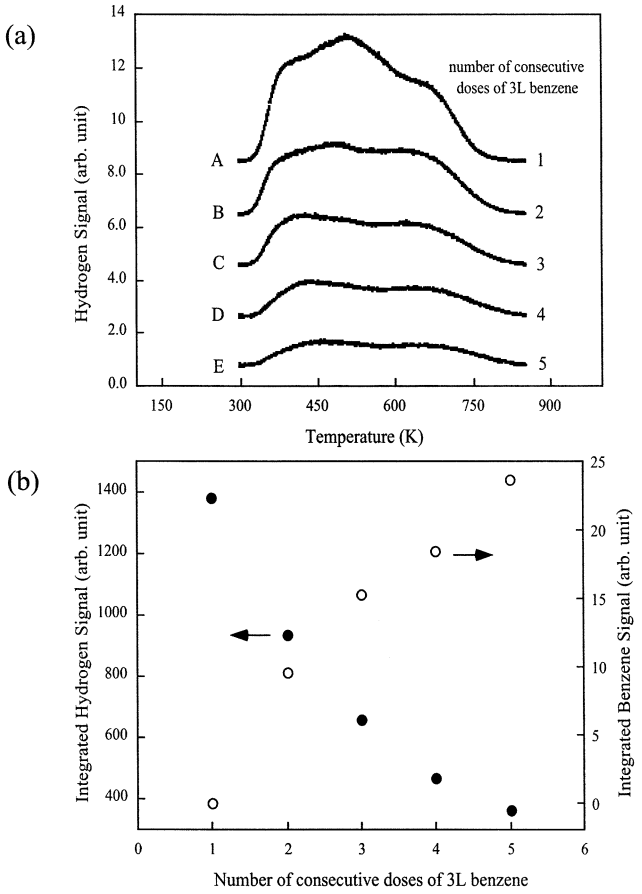

Figure 7. Temperature-programmed desorption spectra of H_2 from adsorption of consecutive doses of 3 langmuirs of C_6H_6 on Ir(210) surface at 300 K (a) and Integrated hydrogen (filled dots) and benzene (open dots) TPD signals versus number of consecutive dose of 3 langmuirs of C_6H_6 on Ir(210) at 300 K (b).

Figure 7a shows a set of H_2 TPD spectra obtained following adsorption of five consecutive doses of 3 langmuirs of C_6H_6 on Ir(210) at 300 K. Similar to the case of C_2H_2 in Figure 6, five H_2 TPD spectra in Figure 7a are obtained under different surface conditions: A is obtained for 3 langmuirs of C_6H_6 on clean Ir(210); after A, the surface is cooled to 300 K and exposed again to 3 langmuirs of C_6H_6, and spectrum B is measured, etc.; after obtaining D, we dose 3 langmuirs of C_6H_6 again and measure spectrum E. No desorption of C_6H_6 is observed from 3 langmuirs of C_6H_6 adsorption on clean Ir(210) at 300 K, which indicates that complete decomposition of benzene is highly favored. This is in contrast to C_6H_6/Ir(111) and C_6H_6/Ir(755)[35] as well as C_6H_6/Ir(110),[40] where the amount of desorbing C_6H_6 is of the same order of magnitude as the amount of desorbing H_2. This implies that the atomically rough Ir(210) surface is much more active than Ir(111), Ir(755), and Ir(110) surfaces in breaking C−H bonds. It is worth mentioning that a small amount of C_6H_6 is seen during measurements of spectra B, C, D, and E, i.e., when the Ir(210) surface is covered by carbon deposit, but is not seen during the measurement of spectrum A (Figure 7b, filled squares).

As seen in Figure 7a (curve A), there are multiple desorption peaks of H_2 from 3 langmuirs of C_6H_6 on clean Ir(210) that extend to temperatures higher than 700 K as a result of thermal decomposition of benzene. This implies that the desorption of H_2 from decomposition of benzene is reaction-rate limited, since all adsorbed H_2 desorbs from the clean Ir(210) surface completely at ~500 K (see Figure 3). The profile of the H_2 TPD

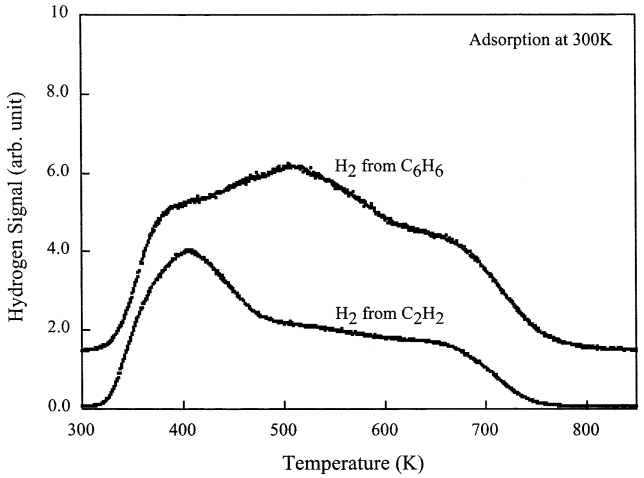

Figure 8. Comparison of temperature-programmed desorption spectra of H_2 from adsorption of 3 langmuirs of C_6H_6 with 3 langmuirs of C_2H_2 on Ir(210) surface at 300 K.

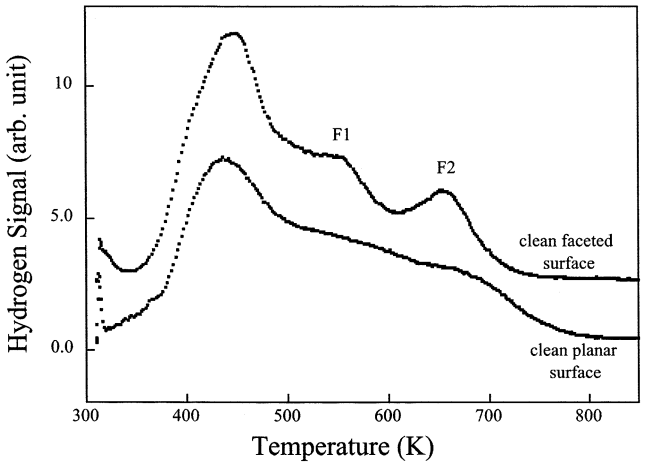

Figure 9. Temperature-programmed desorption spectra of H_2 from clean planar Ir(210) surface and clean faceted Ir(210) surface respectively, which are preexposed to 3 langmuirs of C_2H_2 at 300 K.

spectrum obtained for 3 langmuirs of C_6H_6 on clean Ir(210) (curve A in Figure 7a) is different from that for 3 langmuirs of C_2H_2 on clean Ir(210) (curve A on upper panel in Figure 6), which is directly compared in Figure 8. There are three prominent peaks around ~380, ~500, and ~670 K in the case of C_6H_6, while the dominant peak is located at ~400 K in the case of C_2H_2. In fact, the most substantial difference between two curves is the peak at ~500 K; the two curves are similar at low T (below ~400 K) and high T (above ~650 K). This indicates that there are similarities and differences for the decomposition pathways of C_6H_6 and C_2H_2 on Ir(210).

It is most likely that at low temperatures both C_6H_6 and C_2H_2 undergo partial decomposition to produce hydrocarbon fragments and H atoms with the latter recombining to desorb as H_2 at ~400 K. But above 400 K, the decomposition processes for C_6H_6 and C_2H_2 are dominated by different carbon-containing species that undergo different decomposition pathways. In addition, self-poisoning in the two cases is also different. For C_6H_6, the intensity of the peak around 500 K decreases faster than other peaks as the number of consecutive dose increases (see Figure 7a). In the case of C_2H_2, the intensity of the peak at lowest temperature decreases rapidly as number of consecutive dose increases.

The reactivity of the surfaces toward decomposition of benzene after cycle(s) of dose/TPD dramatically decreases in comparison with clean Ir(210). This observation is reflected by the reduction of integrated H_2 TPD signals resulting from thermal decomposition of benzene, as shown in Figure 7b (dots); this is attributed to a site-blocking effect.

3.2.4. C_2H_2 on Faceted Ir(210). The H_2 TPD spectrum from 3 langmuirs of C_2H_2 on the clean faceted Ir(210) surface is illustrated in Figure 9, where the H_2 TPD spectrum from 3 langmuirs of C_2H_2 on the clean planar Ir(210) surface is also displayed for comparison; in both cases, the adsorption temperature is 300 K. The two pronounced peaks denoted as "F1" and "F2" between 500 and 700 K are unique features of the H_2 TPD curves from C_2H_2 on the faceted Ir(210) surface. The striking difference in TPD spectra of H_2 from decomposition of acetylene on these two types of surfaces can be associated with the introduction of nanometer scale facets on the faceted surface, which illustrates that the decomposition of acetylene is structure sensitive. Note that the change from clean planar Ir(210) to clean faceted Ir(210) involves only a change in local surface geometric structure. These results demonstrate that the changes in local geometric structure at the nanometer scale can play an important role in reaction kinetics in acetylene reactions.

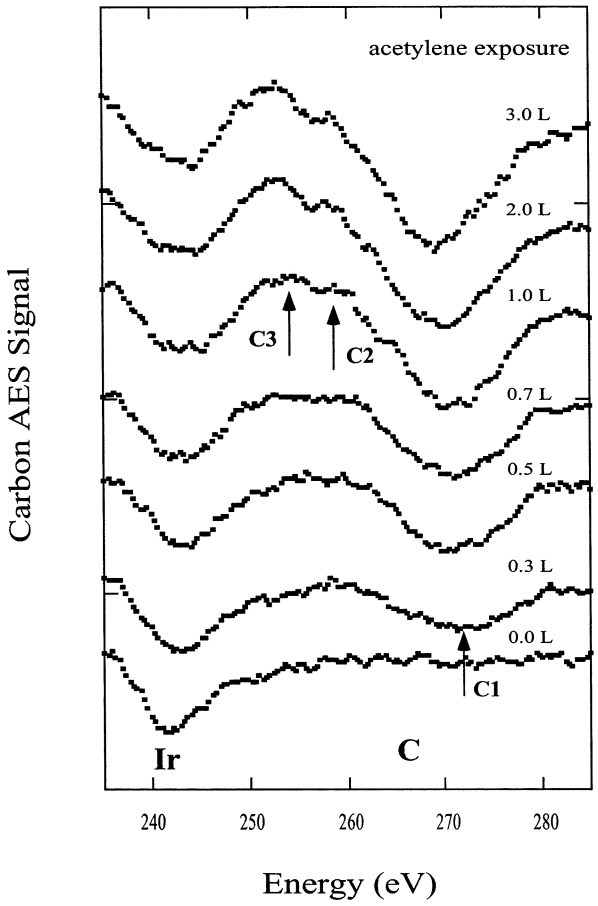

Figure 10. Carbon AES spectra as a function of exposure of C_2H_2 on Ir(210) surface at 300 K. "C1", "C2", and "C3" are three carbon features corresponding to "valley" and "protrusions", respectively.

3.3. Surface Characterization. *3.3.1. AES Measurements.* The carbon KVV AES line shapes are very sensitive to valence electronic structure and are expected to be different for different surface intermediates.[31] We report here in Figures 10 and 11 measurements of carbon KVV AES line shapes as a function of C_2H_2 exposure and annealing temperature. At this stage, these are "fingerprint" measurements to be followed by HREELS

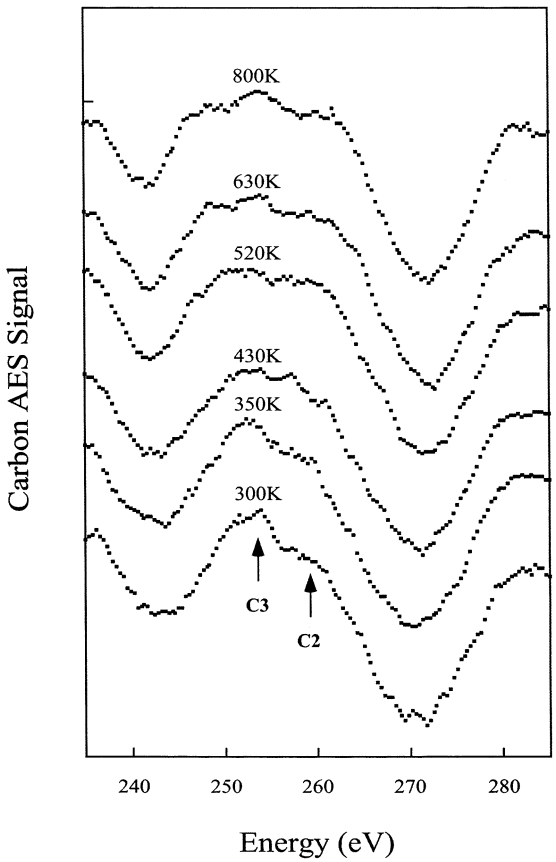

Figure 11. Carbon AES spectra obtained after Ir(210), preexposed to 3 langmuirs of C_2H_2 at 300 K, heated to different temperatures, showing carbon Auger line shape changes at different stages of the reaction. "C2" and "C3" are carbon features (protrusions) and are the same as those in Figure 10.

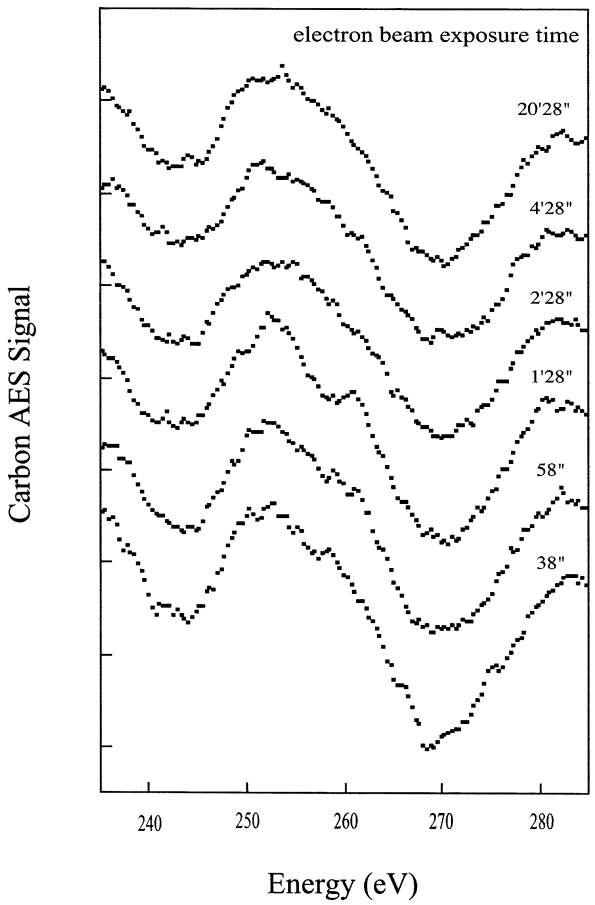

Figure 12. AES spectra of carbon from Ir(210) preexposed to 3 langmuirs of C_2H_2 at 300 K as a function of exposure time to electron beam.

measurements. We are aware of the fact that beam damage can be a problem during AES measurements, and therefore, we tried our best to minimize electron dose. The total e^- exposure in our AES measurements of Figures 10 and 11 does not exceed $\sim 7 \times 10^{15}$ electrons/cm^2; e^- exposure is increased for the beam damage studies of Figure 12.

3.3.1.1. Surface at Different Acetylene Coverage. The carbon AES spectra for different exposures of C_2H_2 on Ir(210) at 300 K are shown in Figure 10. Both the overall appearance of the carbon Auger peak shape and the associated fine structure change dramatically from low to high C_2H_2 exposures, suggesting the formation of different chemical configurations of carbon for adsorbed species on Ir(210). The multiple carbon features appearing at high acetylene exposure provide evidence for multiple carbon-containing species formed on Ir(210) at high coverage. There are three distinct carbon features that develop as a result of acetylene adsorption, denoted as "C1", "C2", and "C3" (see Figure 10). The "C1" feature (seen as a valley) appears on C_2H_2-dosed Ir(210) and grows monotonically as exposure increases. The "C2" and "C3" features (seen as a prominences) are observed for ≥ 1.0 langmuir of C_2H_2 on Ir(210) and also increase with exposure. The differences in the Auger line shape and fine structure at low and high acetylene exposure are ascribed to the formation of different carbon-containing species on Ir(210) surface upon adsorption of acetylene. Note that the Ir(171) peak intensity decreases while C(272) peak intensity increases as the exposure of C_2H_2 increases. For comparison, the carbon AES signals have been normalized to the Ir(171 eV) peaks, i.e., the intensities of displayed Ir(171) peaks in all curves are made to have the same intensity so that the intensity of the carbon features for different exposures of acetylene can be directly compared.

The above observation of change in both the line shape and associated fine structure of carbon Auger spectra provides evidence that AES can be employed to monitor the change in adsorption state of acetylene on Ir(210) surface. This conclusion is supported by the observation in HREELS measurements of different surface hydrocarbon species formed on Ir(210) at high coverage from those at low coverage upon adsorption of acetylene, as described in section 3.3.2.

3.3.1.2. Surface at Different Stages of Reaction. Figure 11 presents the carbon AES spectra of 3 langmuirs of C_2H_2 on clean Ir(210) after annealing to various temperatures corresponding to different stages of the reaction, i.e., as dosed at 300 K followed by annealing. The carbon Auger line shape is very dependent upon the stage of the reaction. The most noticeable changes in the carbon Auger lines are in the region of the "C2" and "C3" features as a function of annealing temperature: both the overall Auger line shape and the associated fine structure are substantially changed above $\sim$520 K. This is attributed to the coexistence of the accumulated carbon-containing species resulting from thermal decomposition of acetylene on Ir(210). The dependence of the carbon Auger spectrum on annealing temperature in the region ≤ 20 K strongly suggests that there are active carbon-containing species involved in the decomposition of acetylene on Ir(210) surface whose concentrations vary with reaction temperature.

3.3.1.3. Electron beam effects. To confirm that the AES spectra presented here were not substantially affected by the

TABLE 1: Vibrational Assignments (cm^{-1}) for Acetylide on Ir(210) Surface and Other Transition Metal Surfaces

	0.5 langmuir of C_2H_2 on Ir(210) at 90 K	C_2H_2 on Pd(100) at 450 K[a]	C_2H_2 on Cu(100) at 375 K[b]	C_2H_4 on Ir(111) at 300 K[c]	C_2H_4 on Ni(110) at 300 K[d]	C_2H_4 on Rh(100) at 300 K[e]	C_2H_4 on Ru(001) at 360 K[f]
δ(CH)	791	750	740	800	890	805	750
ν(CC)	1441	1340	1440	1260	1290	1305	1290
ν(CH)	2949	3000	3020	2960	2990	3025	2960

[a] Kesmodel, L. L; Waddill, G. D.; Gates, J. A. *Surf. Sci*. **1984**, *138*, 464. [b] Marinova, Ts. S.; Stefanov, P. K. *Surf. Sci*. **1987**, *191*, 66. [c] Marinova, Ts. S.; Kostov, K. L. *Surf. Sci*. **1987**, *181*, 573. [d] Stroscio, J. A.; Bare, S. R.; Ho, W. *Surf. Sci.* **1984**, *148*, 499. [e] Slavin, A. J.; Bent, B. E.; Kao, C. T.; Somorjai, G. A. *Surf. Sci*. **1988**, *206*, 124. [f] Hills, M .M.; Parmeter, J. E.; Mullins, C. B.; Weinberg, W. H. *J. Am. Chem. Soc*. **1986**, *108*, 3554.

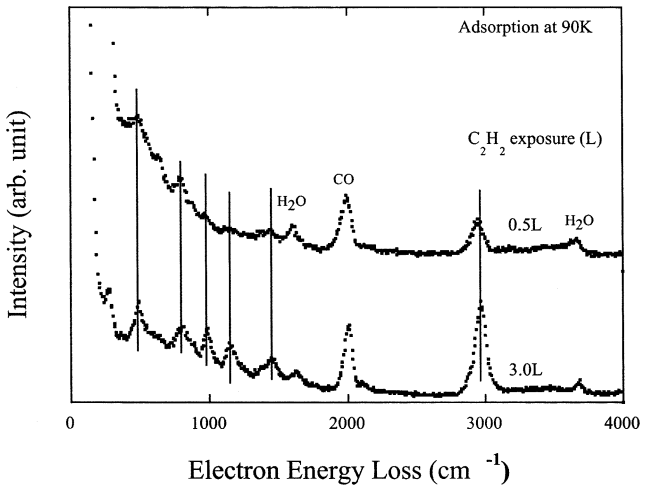

Figure 13. HREEL spectra from Ir(210) surface preexposed to 0.5 and 3.0 langmuirs of C_2H_2 at 90 K, respectively.

electron beam, we expose acetylene-covered Ir(210) to the electron beam for various times before each AES scan. Figure 12 shows the carbon AES spectra for 3 langmuirs of C_2H_2 on clean Ir(210) at 300 K, which has been exposed to the electron beam for different times. Note that these spectra are from different experiments, i.e., the sample has been cleaned before each C_2H_2 dose and AES measurement. Therefore, the spectra shown in Figure 12 indicate that the most significant change in both line shape and associated fine structure of the carbon Auger spectra is observed after the electron beam is on for >88 s, whereas the corresponding changes are insignificant when total exposure time for C_2H_2/Ir(210) to electron beam is ≤88 s. For all carbon AES spectra presented in Figures 10 and 11, the total exposure time to the e^- beam is ~38 s (10s before the AES scan and 28s for the AES scan), giving a total exposure $\sim 7 \times 10^{15} e^-/cm^2$. We suggest that electron-beam induced effects on the AES data of Figures 10 and 11 are negligible. For all carbon AES spectra used to generate the data in Figure 4, the total exposure time to the e^- beam is small enough that electron-beam-induced effects are negligible.

3.3.2. HREELS Measurements. 3.3.2.1. Coverage Dependence. Figure 13 displays the HREEL spectra from the Ir(210) surface preexposed to 3 and 0.5 langmuirs of acetylene at 90 K, respectively. There are substantial differences between the spectra in the two cases. All observed loss features at low coverage (0.5 langmuir) appear at high coverage (3 langmuirs) together with new loss features. This strongly indicates that the surface hydrocarbon species formed at high coverage consist of at least two different fragments: one species is formed at low coverage and the additional species appears as coverage increases.

Following adsorption of 0.5 langmuir of acetylene on clean Ir(210) at 90 K, the dominant acetylene-induced loss features are characterized by peaks at ~791, ~1441, and ~2949 cm^{-1}. These vibrational frequencies are assigned to the fingerprint of acetylide (CCH) on the Ir(210) surface. The assignment is based on a detailed comparison with the characteristic loss features of acetylide (CCH) from C_2H_2 or C_2H_4 on other Ir surfaces[41] and other transition metal surfaces,[42−46] as shown in Table 1. When 3 langmuirs of acetylene is adsorbed on Ir(210) at 90 K, the acetylide loss features persist, and new features appear at ~988, ~1136, ~1448, and ~2970 cm^{-1}. The observed vibrational frequencies are attributed to acetylide combined with ethylidyne (CCH_3). The fingerprint of ethylidyne on Ir(210) is assigned to the new features at ~988, ~1136, ~1448, and ~2970 cm^{-1}. The assignments are based on a comparison with HREELS data of ethylidyne from C_2H_2 or C_2H_4 on other Ir surfaces[47] and other transition metal surfaces,[48,49,50] as well as for an organometallic complex,[51] as summarized in Table 2. Note that the vibrational features for CO (~1996 cm^{-1} at low coverage and ~2009 cm^{-1} at high coverage) and H_2O (~1610, ~3667 cm^{-1} at low coverage and ~1625 cm^{-1}, ~3679 cm^{-1} at high coverage) are seen in both spectra and are ascribed to background gas adsorption during HREELS measurements.[52−56]

3.3.2.2. Clean Faceted Ir(210) versus Clean Planar Ir(210). Figure 14 compares HREEL spectra from adsorption of 3 langmuirs of C_2H_2 on clean planar Ir(210) (left) and clean faceted Ir(210) (right) followed by their thermal evolution up to 500 K. Essentially, all loss features observed on clean planar Ir(210) can be seen on clean faceted Ir(210) with varied intensities, indicating that similar surface hydrocarbon species are formed on both clean planar and clean faceted Ir(210) surfaces upon adsorption at 90 K. When C_2H_2-covered Ir is heated to 300, 400, and 500 K, a similar thermal behavior is observed as evidenced by the simultaneous growth of peaks located at certain frequencies and simultaneous weakening or disappearance of the peaks at other frequencies. All this strongly indicates that the surface hydrocarbon species formed upon adsorption of acetylene are similar on both planar and faceted Ir(210) and that their thermal decomposition behaviors are also similar at ≤500 K. This finding is consistent with TPD results which show that the H_2 TPD spectra from acetylene on clean planar and clean faceted Ir(210) (Figure 9) differ significantly only above 500 K. A more detailed HREELS study is planned to explore the decomposition pathways above 500 K on the two surfaces.

4. Discussion

Nieuwenhuys et al. found that H_2 is the only TPD product from Ir(111) and Ir(755) when C_2H_2 is adsorbed on these two surfaces at 303 K,[35] whereas the amount of desorbing C_6H_6 is of the same order of magnitude as the amount of desorbing H_2

TABLE 2: Vibrational Assignments (cm^{-1}) for Ethylidyne on Ir(210) Surface and Other Transition Metal Surfaces

	3 langmuirs of C_2H_2 on Ir(210) at 90 K	C_2H_4 on Ir(111) at 180 K[a]	C_2H_4 on Ir(110) at 170 K[a]	C_2H_4 on Pd(111) at 150 K[b]	C_2H_2 on Ru(001) at 330 K[c]	$(CO)_9Co_3(CCH_3)$ at 300 K[d]	C_2H_4 on C/Mo(110) at 260 K[e]
ρ(CH)	988	980	980	914	970	1004	920
ν(CC)	1136	1165	1158	1080	1120	1163	1075
δ(CH)	1448	1400	1400	1334	1450	1356	1345
					1340	1420	1430
ν(CH)	2970	2950	2935	2900	2910	2888	2915
					3000	2930	

[a] Chakarov, D. V.; Marinova, Ts. *Surf. Sci*. **1990**, *227*, 297. [b] Gates, J. A.; Kesmodel, L. L. *Surf. Sci*. **1983**, *124*, 68. [c] Jakob, P.; Cassuto, A.; Menzel, D. *Surf. Sci*. **1987**, *187*, 407. [d] Skinner, P.; Howard, M. W.; Oxton, I. A.; Kettle, S. F. A.; Powell, D. B.; Sheppard, N. *J. Chem. Soc., Faraday Trans.* **1981**, *2*, 77. [e] Frühberger, B.; Chen, J. G. *J. Am. Chem. Soc.* **1996**, *118*, 11599.

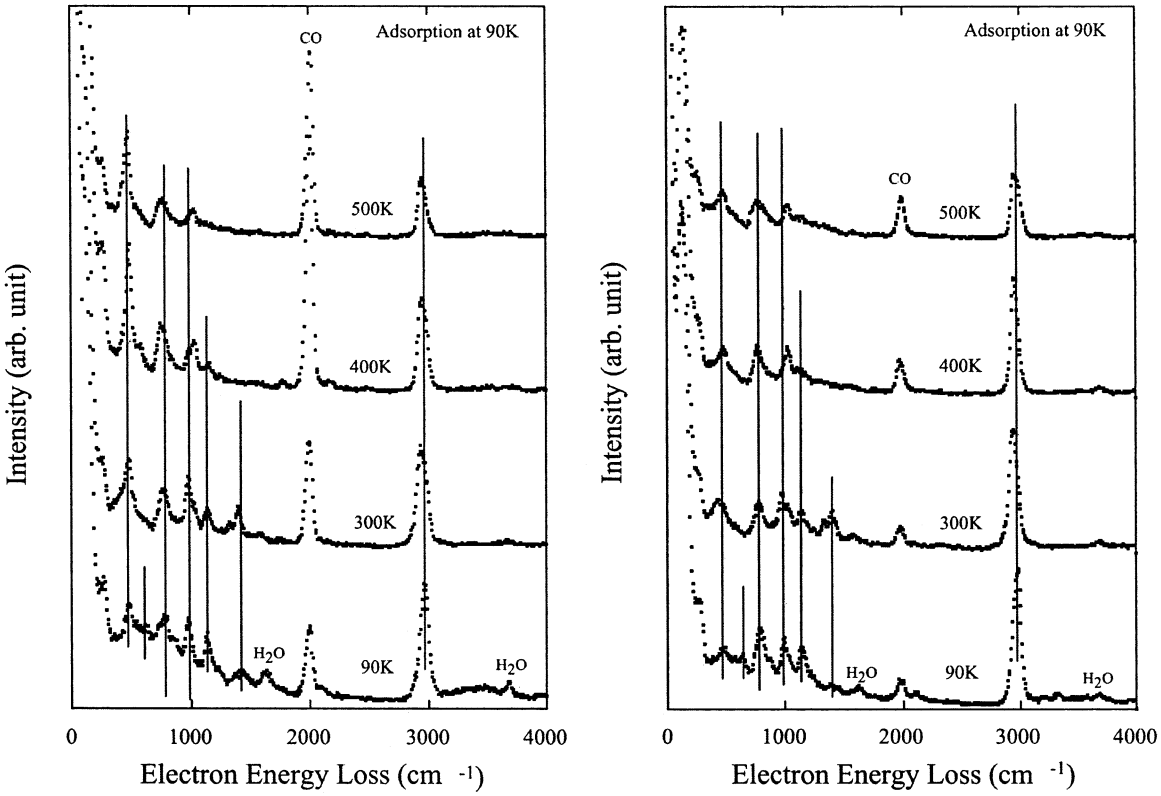

Figure 14. HREEL spectra for 3 langmuirs of C_2H_2 dose at 90 K and annealing sequence on clean planar Ir(210) (left) and clean faceted Ir(210) (right). All spectra were recorded at 90 K.

when C_6H_6 is adsorbed on these two surfaces at 303 K. Nieuwenhuys and Somorjai[40] also found that the amount of desorbing C_6H_6 is of the same order of magnitude as the amount of desorbing H_2 when C_6H_6 is adsorbed on Ir(110) at 303 K. Using HREELS, Marinova and Kostov[41] demonstrated that C_2H_2 is adsorbed as CCH (acetylide) and CCH_3 (ethylidyne) species on an Ir(111) surface preexposed to C_2H_2 at either 180 or 300 K. After C_2H_2-covered Ir(111) is heated to 500 K, the ethylidyne completely decomposes to CCH species. In addition, they found that, upon adsorption of C_2H_2, the formation of CCH species on Ir(111) occurs mostly at low coverage while ethylidyne species are observed at higher coverage. In this work, the reaction pathway for C_2H_2/Ir(210) is decomposition instead of self-hydrogenation to ethylene and cyclization to benzene, which is similar to that for C_2H_2/Ir(111) and Ir(755). The two different kinds of carbon-containing surface species [acetylide (CCH) and ethylidyne (CCH_3)] formed on Ir(111) upon adsorption of C_2H_2 are also observed on Ir(210) upon adsorption of C_2H_2. The main difference between our work and previous work on the adsorption of C_6H_6 on other Ir crystal surfaces is that the complete decomposition of C_6H_6 on Ir(210) occurs while the amount of desorbing C_6H_6 is of the same order of magnitude as the amount of desorbing H_2 for C_6H_6/Ir(111), C_6H_6/Ir(755), and C_6H_6/Ir(110). The detailed comparison is described below.

4.1. Reaction of C_2H_2 on Ir(210). When the acetylene-covered Ir(210) is heated to elevated temperatures, the dominantdesorption product is hydrogen, indicating that the Ir(210) surface is highly active for decomposition of C_2H_2 to H_2 rather than cyclization to C_6H_6 or self-hydrogenation to C_2H_4, which is similar to the behaviors of C_2H_2/Ir(111) and C_2H_2/Ir(755); the cyclization or self-hydrogenation of acetylene does not occur on either of these surfaces.[35]

When the acetylene-covered Ir(210) is heated to temperatures higher than 500 K, the desorption of H_2 from the surface continues to occur (Figure 5), whereas all adsorbed H_2 on the clean Ir(210) surface desorbs completely below 500 K (Figure 3). In addition, the typical H_2 TPD spectrum from C_2H_2/Ir(210) is asymmetric at low coverage and broadens toward both lower and higher temperatures with increasing coverage (Figure 5) but the H_2 TPD curve from H_2/Ir(210) broadens only toward

lower temperatures with increasing coverage (Figure 3). These indicate that the H_2 desorbed from C_2H_2/Ir(210) during TPD is reaction-rate limited.

As seen in Figure 5, the H_2 TPD curve from C_2H_2/Ir(210) becomes broader with the appearance of additional features on the high-temperature side (>500 K) with increasing exposures of C_2H_2. This implies that the decomposition of acetylene on Ir(210) occurs in a stepwise fashion, possibly due to further decomposition of the surface intermediates resulting from thermal decomposition of adsorbed carbonaceous species on the surface upon adsorption of acetylene. The concentration of adsorbed carbonaceous species, which we denote as "high-coverage species (HCS)", seems to increase as a function of acetylene exposure. This HCS is associated with the carbon AES features "C2" and "C3" that grow with increasing coverage of acetylene (Figure 10); these features decrease with increased annealing temperature (Figure 11) due to decreased concentration resulting from thermal decomposition. Our HREELS data (Figure 13 and Tables 1 and 2) indicate that the HCS formed at saturation overage of acetylene (3 langmuir dose) is a combination of acetylide with ethylidyne while the adsorbed carbonaceous species formed at low coverage (0.5 langmuir dose), which we denote as "low-coverage species (LCS)", is acetylide. It is the ethylidyne species that increase in concentration with acetylene coverage. When C_2H_2/Ir(210) is annealed, both HCS and LCS decompose to produce H_2, and the HCS also decomposes to produce other intermediate species that undergo further decomposition at higher temperatures to produce H_2 and leave C on the surface. Similar results from HREELS have been reported for C_2H_2 on Ir(111).[41]

The fact that cyclization of acetylene to benzene does not occur on the Ir(210) surface is in contrast to the measurements on an Ir organometallic complex.[34] It is believed that cyclization of acetylene to benzene proceeds through a stepwise process with the rate-determining step being the addition of acetylene to a C_4H_4 intermediate.[1,7,11] The difference between an Ir organometallic complex and the Ir surface is that there is only a single Ir atom in the complex while each Ir atom on the surface is surrounded by neighboring Ir atoms. Therefore, the single Ir atom in the complex can stabilize the C_2H_2 and facilitate the coupling of two C_2H_2 species to form C_4H_4, while the Ir crystal surface provides a good template for C_2H_2 dissociation due to the availability of more Ir sites.

4.2. Comparison of C_2H_2/Ir(210) with C_6H_6/Ir(210). When the acetylene-covered Ir(210) and benzene-covered Ir(210) (adsorption at 300 K) are heated, the dominant desorption product is hydrogen, and its desorption is reaction-rate limited in both cases. Although C_6H_6 and C_2H_2 both decompose on Ir(210), the H_2 TPD curve for C_6H_6/Ir(210) has a different character from that for C_2H_2/Ir(210) as seen in Figure 8. The curves in Figure 8 are similar at low T ($\leq$400 K) and high T ($\geq$650 K) but different at intermediate T. This indicates that the decomposition pathways exhibit both similarities and differences. The dominant feature in the case of C_2H_2 is at ~400 K, while the dominant feature in the case of C_6H_6 is at ~500 K, although in both cases the dominant feature reduces much faster than others as surface reactivity decreases (Figures 6a and 7a). The similarities at $T \leq 400$ K may indicate that both benzene and acetylene undergo partial decomposition to produce atomic hydrogen and hydrocarbon intermediates, whereas the higher temperature evolution of TPD spectra (Figure 8) is a consequence of different decomposition pathways of the surface hydrocarbon intermediates. This merits further study.

Note that, during the heating of the saturation coverage of acetylene or benzene covered surfaces, we did not observe evidence for formation of carbide compounds on either planar or faceted surfaces.[68] The carbon Auger line shape after heating C_2H_2/Ir or C_6H_6/Ir indicates that residual surfaces carbon is graphite-like.

4.3. Structure Sensitivity in C_2H_2/Ir(210). Although the clean Ir(210) surface has a planar (1 × 1) structure, it is morphologically unstable when covered with oxygen and heated. When Ir(210) is exposed to more than ~0.9 langmuir of O_2 and annealed to temperatures higher than 600 K, the initially planar Ir(210) surface becomes faceted: three-sided pyramid-like structures are formed on the initially planar Ir(210) surface as revealed by LEED and STM.[25,26] We are able to remove the surface oxygen via catalytic reaction with CO or with H_2, but the surface still remains faceted. The distinct differences in H_2 TPD spectra, especially between 500 and 700 K for acetylene-covered clean planar Ir(210) and faceted Ir(210) as compared in Figure 9, provide strong evidence for structure sensitivity in the decomposition of acetylene over Ir surfaces. This structure sensitivity is manifested in desorption from nanometer scale surface structures on the faceted surface. Similar structure sensitivity in acetylene reactions over planar and faceted Pd/W(111) has been published previously,[12] although the reaction pathways are different from that on Ir surfaces. It should be noted that, unlike the faceted W(111) surface induced by Pd (which has three-sided pyramidal facets having only {211} faces,[23] the faceted Ir(210) surface induced by oxygen has facets with two different kinds of faces (two {311} faces and one {110} face).[25,26] The presence of two faces on the nanometer scale may make the surface reactions more complicated due to kinetic competition and finite size effects.[57] A detailed study of acetylene reactions over faceted Ir(210) surface will be reported elsewhere.[58]

Using Monte Carlo simulations, Persson et al.[59] have recently investigated the interplay between the reactions on adjacent facets of nanometer-sized supported catalyst particles. The results indicate that the reaction kinetics on faceted nanocrystals can be remarkably different from those on single-crystal surfaces due to nontrivial coupling of the kinetics of the individual facets. Earlier experimental studies of acetylene reactions over Pd/W(111)[12] reveal the important effects of geometric structure and finite size at the nanometer scale when the faceted surface consists of facets having only one face as compared to two different faces in the present study.

4.4. Comparison of Ir(210) with Other Iridium Crystal Faces. Comparison of our TPD data for C_6H_6/Ir(210) with those for C_6H_6/Ir(111), C_6H_6/Ir(755),[35] and C_6H_6/Ir(110)[40] leads to the conclusion that the Ir(210) surface is more active than Ir(111), Ir(755), and Ir(110) surfaces in breaking C−H bonds for decomposition of benzene. The higher reactivity for the Ir(210) surface over Ir(111), Ir(755), and Ir(110) surfaces might be associated with the presence of low-coordination sites for the surface atoms on Ir(210). Figure 15 displays the top view and side view of Ir(210) surface. The atoms a, b, c, and d are the surface atoms of Ir(210) in the first, second, third, and fourth layers respectively, and their coordination sites are C_6, C_9, C_{11}, and C_{12}, where N denotes the number of nearest-neighbor atoms. Therefore, atomically rough Ir(210) surface contains six-coordination sites C_6 (i.e., six nearest-neighbor atoms), while Ir(110), Ir(755), and Ir(111) surface atoms have no such low-coordination sites. The close-packed Ir(111) surface atoms have only nine-coordination sites C9. The Ir(755) surface consists of (111) terraces separated by steps along the (100) orientation

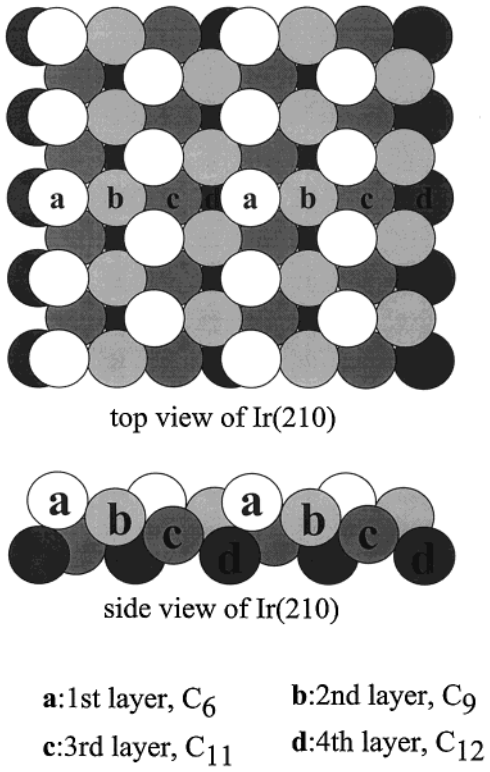

Figure 15. Top view and side view of hard-sphere model of Ir(210) surface showing the coordination numbers C_N of Ir surface atoms. *N* denotes the number of nearest-neighbor atoms.

with a single atom height,[60,61] which contains seven-coordination sites C7 and nine-coordination sites C9. The clean Ir(110) surface reconstructs into a corrugated (1 × 2) superstructure[62] that contains seven-coordination sites C7, nine-coordination sites C9, and eleven-coordination sites C11.[63]

4.5. Model System For Surface Chemistry. The modification of catalytic surfaces induced by various adsorbates has been investigated extensively.[33,64−66] It has been made clear that adsorbate does influence the surface catalytic activity, e.g., a single physical monolayer (ML) of Pd on W(211) decreases the high reactivity toward acetylene decomposition, which proceeds on clean W(211), and catalyzes the cyclization of acetylene.[33] Many studies have shown that the metal particle size as well as strong metal support interaction (SMSI) considerably influence the catalytic activity of the supported metal catalyst.[67] However, the present modification of the Ir(210) surface, i.e., generation of clean faceted Ir(210), avoids the influence of any adsorbate on reaction kinetics, as described below.

Clear evidence for structure sensitivity in decomposition of acetylene over the clean faceted Ir(210) surface versus the clean planar Ir(210) surface is shown in the TPD data (Figure 9). The new surface [clean faceted Ir(210)] having different reactivity with respect to original surface [clean planar Ir(210)] can be easily and routinely prepared in situ. Although O_2 and H_2 are used in the process for the new surface preparation [oxygen is used to remove surface carbon contamination and then generate oxygen-covered faceted Ir(210), while hydrogen is used to remove surface oxygen from oxygen-covered faceted Ir(210) to generate final clean faceted Ir(210)], the resulting new surface, i.e., clean faceted Ir(210), is free of any adsorbate. Moreover, the new catalytic surface contains nanometer scale facets that will help provide insights into the reaction mechanism at the nanometer scale. The nanometer scale facets result in reaction kinetics that are different from those on the planar surface due to the change in surface geometric structure, effects of finite size at nanometer scale, and the interplay of catalytic reactions on different facets.[57,59] The structural modification of catalytic activity of the surface in this way (without adding promoters, poisons, or support material on the surface) may be unprecedented and demonstrates that Ir(210) is an excellent model catalytic system for surface chemistry studies involving structure sensitive reaction.

5. Conclusions

The TPD results presented here clearly exhibit that the Ir(210) surface is very active for dissociation of acetylene to hydrogen; the evolution of H_2 is reaction-rate limited and occurs in a stepwise fashion at higher acetylene exposures. The determining role of the surface reactive intermediates involved in the stepwise reactions is addressed by AES characterization of the surface at different acetylene coverage and at different stages of the reaction. The carbon KVV features at high acetylene coverage provide a fingerprint of the active surface carbon-containing species upon adsorption of acetylene on clean Ir(210) at 300 K, which undergo thermal decomposition upon heating to higher temperatures. HREELS data show that, upon adsorption of acetylene at 90 K, the surface species formed are dominated by acetylide at low coverage and by coexisting acetylide and ethylidyne at high coverage. No benzene desorption is observed from C_2H_2/Ir(210) during TPD, indicating that Ir(210) is inactive for the cyclization of acetylene. C_6H_6 also decomposes to produce H_2 over Ir(210). The reaction sequence for the decomposition of acetylene to hydrogen on Ir(210) exhibits similarities and differences from decomposition of benzene to hydrogen on Ir(210). Ir(210) is more active than Ir(111), Ir(755), and Ir(110) in breaking C−H bonds for the decomposition of benzene. Evidence has been found for structure sensitivity in the decomposition of acetylene over planar and faceted Ir(210) surfaces. The structure sensitivity is influenced by the presence of different facet planes ({311} and {110}) on the faceted surface and by finite size effects.

The combination of adsorption and desorption measurements by TPD with the surface characterization at different acetylene coverage and different stages of the reaction by AES and HREELS is very useful in obtaining new insights into the reaction mechanisms in surface acetylene reactions.

Acknowledgment. We thank Boris Yakshinsky and Robin Barnes for technical assistance in the initial set up of the experiments, and Hao Wang, Ihab M. Abdelrehim, and Kalman Pelhos for helpful discussion. The Rutgers work has been supported in part by US Department of Energy (DOE) Office of Basic Energy Sciences (Grant DE-FG02-93ER14331). J.G.C. and H.H.H. also acknowledge partial support from the DOE Office of Basic Energy Sciences (Grant DE-FG02-00ER15014).

References and Notes

(1) Tysoe, W. T.; Nyberg, G. L.; Lambert, R. M. *Surf. Sci.* **1983**, *135*, 128.
(2) Rucker, T. G.; Logan, M. A.; Gentle, T. M.; Muetterties, E. L.; Somorjai, G. A. *J. Phys. Chem.* **1986**, *90*, 2703.
(3) Marchon, B. *Surf. Sci.* **1985**, *162*, 382.
(4) Avery, N. R. *J. Am. Chem. Soc.* **1985**, *107*, 6711.
(5) Lomas, J. R.; Baddeley, C. J.; Tikhov, M. S.; Lambert, R. M. *Langmuir* **1995**, *11*, 3048.
(6) Dvorak, J.; Hrbek, J. *J. Phys. Chem. B* **1998**, *102*, 9443.
(7) Patterson, C. H.; Lambert, R. M. *J. Am. Chem. Soc.* **1988**, *110*, 6871.
(8) Patterson, C. H.; Lambert, R. M. *J. Phys. Chem.* **1988**, *92*, 1266.

(9) Yoshinobu, J.; Sekitani, T.; Onchi, M.; Nishijima, M. *J. Phys. Chem.* **1990**, *94*, 4269.
(10) Stacchiola, D.; Molero, H.; Tysoe, W. T. *Catal. Today* **2001**, *65*, 3.
(11) Abdelrehim, I. M.; Pelhos, K.; Madey, T. E.; Eng, J., Jr.; Chen, J. G. *J. Mol. Catal. A: Chem.* **1998**, *131*, 107.
(12) Barnes, R.; Abdelrehim, I. M.; Madey, T. E. *Top. Catal.* **2001**, *14*, 53.
(13) Brucker, C.; Rhodin, T. *J. Catal.* **1977**, *47*, 214.
(14) Egawa, C.; Naito, S.; Tamaru, K. *J. Chem. Soc., Faraday Trans.* **1986**, *82*, 3197.
(15) Avery, N. R. *Langmuir* **1988**, *4*, 445.
(16) Klug, C. A.; Slichter, C. P.; Sinfelt, J. H. *Isr. J. Chem.* **1992**, *32*, 185.
(17) Nozoye, H. *Surf. Sci.* **1992**, *269/270*, 335.
(18) Hung, W. H.; Bernasek, S. L. *Surf. Sci.* **1995**, *339*, 272.
(19) Vaari, J.; Lahinen, J.; Hautojärvi, P. *Catal. Lett.* **1997**, *44*, 43.
(20) Eng, J., Jr.; Chen, J. G.; Abdelrehim, I. M.; Madey, T. E. *J. Phys. Chem. B* **1998**, *102*, 9687.
(21) Bhattacharya, A. K.; Pyke, D. R. *J. Mol. Catal. A: Chem.* **1998**, *129*, 279.
(22) Papageorgopoulos, D. C.; Ge, Q.; Nimmo, S.; King, D. A. *J. Phys. Chem. B* **1997**, *101*, 1999.
(23) Nien, C. H.; Madey, T. E. *Surf. Sci.* **1997**, *380*, L527.
(24) Nien, C. H.; Madey, T. E.; Tai, Y. W.; Leung, T. C.; Che, J. G.; Chan, C. T. *Phys. Rev. B* **1999**, *59*, 10335.
(25) Madey, T. E.; Pelhos, K.; Wu, Q.; Barnes, R.; Ermanoski, I.; Chen, W.; Kolodziej, J. J.; Rowe, J. E. *Proc. Natl. Acad. Sci. U.S.A.* **2002**, *99*, 6503.
(26) Ermanoski, I.; Pelhos, K.; Chen, W.; Quinton, J. S.; Madey, T. E. In preparation.
(27) Briggs, D.; Rivière, J. C. in *Practical Surface Analysis*; Briggs, D., Seah, M. P., Eds.; Wiley: New York, 1996; see also references therein.
(28) Kny, E. *J. Vac. Sci. Technol.* **1980**, *17*, 658.
(29) Kleefeld, J.; L. L. Levenson, L. L. *Thin. Solid Films* **1979**, *64*, 389.
(30) Smith, M. A.; Levenson, L. L. *Phys. Rev. B* **1977**, *16*, 1365.
(31) Rye, R. R.; Madey, T. E.; Houston, J. E.; Holloway, P. H. *J. Chem. Phys.* **1978**, *69*, 1504.
(32) Ibach, H.; Mills, D. L. *Electron Energy Loss Spectroscopy and Surface Vibrations*; Academic Press: New York, 1982.
(33) Abdelrehim, I. M.; Pelhos, K.; Madey, T. E.; Eng, J., Jr.; Chen, J. G. *J. Phys. Chem. B* **1998**, *102*, 9697.
(34) Bianchini, C.; Caulton, K. G.; Chardon, C.; Doublet, M. L.; Eisenstein, O.; Jackson, S. A.; Johnson, T. J.; Meli, A.; Peruzzini, M.; Streib, W. E.; Vacca, A.; Vizza, F. *Organometallics* **1994**, *13*, 2010.
(35) Nieuwenhuys, B. E.; Hagen, D. I.; Rovida, G.; Somorjai, *G. A. Surf. Sci.* **1976**, *59*, 155.
(36) Song, K. J.; Dong, C.-Z.; Madey, T. E. *Langmuir* **1991**, *7*, 3019.
(37) Pelhos, K.; Abdelrehim, I. M.; Nien, C.-H.; Madey, T. E. *J. Phys. Chem. B* **2001**, *105*, 3708.
(38) Hwu, H. H.; Chen, J. G.; Kourtakis, K.; Lavin, J. G. *J. Phys. Chem. B* **2001**, *105*, 10037.
(39) Chen, W.; Madey, T. E. In preparation.
(40) Nieuwenhuys, B. E.; Somorjai, G. A. *Surf. Sci.* **1978**, *72*, 8.
(41) Marinova, Ts. S.; Kostov, K. L. *Surf. Sci.* **1987**, *181*, 573.
(42) Kesmodel, L. L.; Waddill, G. D.; Gates, J. A. *Surf. Sci.* **1984**, *138*, 464.
(43) Marinova, Ts. S.; Stefanov, P. K. *Surf. Sci.* **1987**, *191*, 66.
(44) Stroscio, J. A.; Bare, S. R.; Ho, W. *Surf. Sci.* **1984**, *148*, 499.
(45) Slavin, A. J.; Bent, B. E.; Kao, C. T.; Somorjai, G. A. *Surf. Sci.* **1988**, *206*, 124.
(46) Hills, M. M.; Parmeter, J. E.; Mullins, C. B.; Weinberg, W. H. *J. Am. Chem. Soc.* **1986**, *108*, 3554.
(47) Chakarov, D. V.; Marinova, Ts. *Surf. Sci.* **1990**, *227*, 297.
(48) Gates, J. A.; Kesmodel, L. L. *Surf. Sci.* **1983**, *124*, 68.
(49) Jakob, P.; Cassuto, A.; Menzel, D. *Surf. Sci.* **1987**, *187*, 407.
(50) Frühberger, B.; Chen, J. G. *J. Am. Chem. Soc.* **1996**, *118*, 11599.
(51) Skinner, P.; Howard, M. W.; Oxton, I. A.; Kettle, S. F. A.; Powell, D. B.; Sheppard, N. *J. Chem. Soc., Faraday Trans.* **1981**, *2*, 77.
(52) Marinova, Ts. S.; Chakarov, D. V. *Surf. Sci.* **1989**, *217*, 65.
(53) Kisters, G.; Chen, J. G.; Lehwald, S.; Ibach, H. *Surf. Sci.* **1991**, *245*, 65.
(54) Hagedorn, C. J.; Weiss, M. J.; Weinberg, W. H. *J. Phys. Chem. B* **2001**, *105*, 3838.
(55) Thiel, P. A.; Madey, T. E. *Surf. Sci. Rep.* **1987**, *211*, 7.
(56) Hwu, H. H.; Polizzotti, B. D.; Chen, J. G. *J. Phys. Chem. B* **2001**, *105*, 10045.
(57) Zhdanov, V. P.; Kasemo, B, *Surf. Sci. Rep.* **2000**, *39*, 29 and references therein.
(58) Chen, W.; Madey, T. E.; et al. In preparation.
(59) Persson, H.; Thormahlen, P.; Zhdanov, V. P.; Kasemo, B. *J. Vac. Sci. Technol., A* **1999**, *17*, 1721 and references therein.
(60) Rokuta, E.; Hasegawa, Y.; Itoh, A.; Yamashita, K.; Tanaka, T.; Otani, S.; Oshima, C. *Surf. Sci.* **1999**, *427*, 27.
(61) Somorjai, G. A. *Introduction to Surface Chemistry and Catalysis*; John Wiley & Sons: New York, 1994.
(62) Chan, C. M.; Van Hove, M. A.; Weinberg, W. H.; Williams, E. D. *Solid State Commun.* **1979**, *30*, 47.
(63) Engstrom, J. R.; Goodman, D. W.; Weinberg, W. H. *J. Am. Chem. Soc.* **1988**, *110*, 8305, and references therein.
(64) Baddeley, C. J.; Tikhov, M.; Hardacre, C.; Lomas, J. R.; Lambert, R. M. *J. Phys. Chem.* **1996**, *100*, 2189.
(65) Logan, M. A.; Rucker, T. G.; Gentle, T. M.; Muetterties, E. L.; Somorjai, G. A. *J. Phys. Chem.* **1986**, *90*, 2709.
(66) Xu, C.; Peck, W.; Koel, B. E. *J. Am. Chem. Soc.* **1993**, *115*, 751.
(67) Baker, R. T. K.; Tauster, S. J.; Dumesic, J. A. *Strong Metal-Support Interactions*; ACS Symposium Series 298; American Chemical Society: Washington, DC, 1986; see also references therein.
(68) Kelley, R. D. and Goodman, D. W. In *The Chemical Physics of Solid Surfaces and Heterogeneous Catalysis*; King, D. A., Woodruff, D. P., Eds.; Elsevier: The Netherlands, 1982; Vol. 4.